Available online at www.sciencedirect.com

SciVerse ScienceDirect

Ceramics International 39 (2013) 2077–2081

CERAMICS INTERNATIONAL

www.elsevier.com/locate/ceramint

Fabrication of porous spinel ($MgAl_2O_4$) from porous alumina using a template method

Shinobu Hashimoto*, Sawao Honda, Tomoki Hiramatsu, Yuji Iwamoto

Department of Environmental and Materials Engineering, Nagoya Institute of Technology, Gokiso-cho, Nagoya 466–8555, Japan

Received 3 July 2012; received in revised form 21 August 2012; accepted 23 August 2012
Available online 31 August 2012

Abstract

A porous spinel body was fabricated from porous alumina using a template method. First, alumina with 72.5% porosity was fabricated by heating a compact from platelets at 1400 °C for 1 h. The resultant porous alumina was then immersed in an 8 mol/L magnesium nitrate solution, dried, and reheated at 1400 °C for 2 h to convert it to spinel. If necessary, this solution immersion and reheating treatment was performed up to five times. The influence of the number of treatments on the porosity, conversion ratio to spinel, compressive strength, and thermal conductivity was investigated. After five solution treatments, the conversion ratio to spinel was calculated to be approximately 30% in molar ratio, while the remaining majority maintained the morphology of the original alumina platelets. The porosity, compressive strength, and thermal conductivity of the final sample at room temperature were 61.0%, 13.0 MPa, and 1.8 $Wm^{-1}K^{-1}$, respectively.

Keywords: Porous spinel; Template method; Compressive strength

1. Introduction

Magnesium aluminate spinel ($MgAl_2O_4$) has excellent properties, including a high melting point (2135 °C), low thermal conductivity, low thermal expansion [1], and high corrosion resistance [2], and so it is expected to be appropriate for use in refractory materials. However, spinel formation by the solid phase reaction between MgO and Al_2O_3 is slow [3], so an extended reaction time and/or high temperatures are necessary to complete the spinel formation process. In addition, spinel formation from MgO and Al_2O_3 is accompanied by a 5–7% volume expansion [4], resulting in low sinterability. Generally, a two-step process is employed for the fabrication of dense spinel bodies. The first step is the formation of a fine, active spinel powder, and the second is the sintering of a spinel fine powder compact. Therefore, techniques such as high-energy ball milling or attrition milling of a pre-synthesized spinel powder have been used before the final sintering process [5,6]. Furthermore, in order to fabricate a fine spinel powder with high sinterability, synthesis methods such as spray pyrolysis [7,8], freeze-drying [9], hydroxide coprecipitation [10], and the use of metal alkoxide sol–gels [11] have been developed.

Recently, porous ceramics have been proposed as refractory materials for high-temperature industrial manufacturing. These porous ceramics could easily withstand higher temperatures in high-temperature facilities, which would lead to lower energy costs for heating. Particularly, porous spinel is an attractive material for the steel-making industry. However, only a few studies on porous spinel ceramics have been reported [12]. In an attempt to fabricate porous spinel with high-performance properties such as high porosity, high strength, and low thermal conductivity, a novel template method using a porous alumina body was adopted. First, porous alumina was fabricated from platelets in order to increase the porosity [13]. Subsequently, the resultant porous alumina was immersed in a magnesium nitrate solution, dried, and then reheated at high temperatures to undergo transformation into spinel, while maintaining the porosity.

---

*Corresponding author.
E-mail address: hashimoto.shinobu@nitech.ac.jp (S. Hashimoto).

0272-8842/$ - see front matter © 2012 Elsevier Ltd and Techna Group S.r.l. All rights reserved.
http://dx.doi.org/10.1016/j.ceramint.2012.08.062

This solution immersion and reheating treatment was performed repeatedly.

In this study, the influence of the number of magnesium nitrate solution and reheating treatments (hereafter referred to as solution treatments) on the porosity, compressive strength, spinel conversion rate, and thermal conductivity of the resultant porous samples were investigated.

2. Experimental procedure

Commercial alumina platelets (SERAF: YFA05025, Kinseimatech Co. Ltd., Japan) with a 4.6 μm average diameter, an aspect ratio of 20 and 99.2% purity were used, as shown in Fig. 1 and Table 1. Fine alumina (Taimicron, 0.14 μm in diameter and 99.9% pure, Taimei-kagaku Co. Ltd., Japan) was used as a sintering additive. Corn starch (10 μm, Kishidakagaku Co. Ltd., Japan) was also added to the starting materials as a pore former. Reagent-grade magnesium nitrate hydrate (Kishidakagaku Co. Ltd., Japan) was dissolved in distilled water to prepare an 8 mol% solution. A powder mixture consisting of alumina platelets: fine alumina: corn starch = 85: 10: 5 (mass%) was uniaxially pressed at 1 MPa to form a 10 mm diameter × 20 mm high cylindrical green compact. This compact was heated at 1400 °C for 1 h to form a porous alumina body. Subsequently, the resultant porous alumina body was immersed into the above magnesium nitrite solution for 1 h under vacuum, removed, and then dried at room temperature for 24 h. The resultant sample was reheated at 1400 °C for 2 h in air. This solution immersion and reheating treatment was performed up to five times.

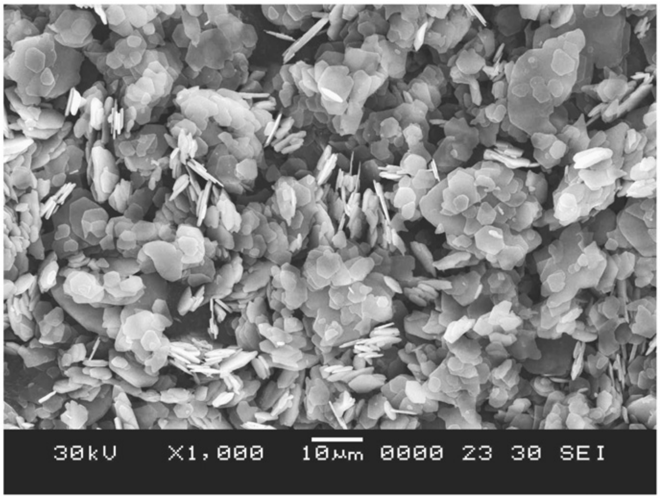

Fig. 1. SEM micrograph of the α-alumina platelets used.

Table 1
Characteristics of starting α-alumina platelets.

Average grain size	4.6 μm
Average aspect ratio	20
Composition	mass%
Al_2O_3	99.2
Na_2O	0.23
SiO_2	0.06
Fe_2O_3	0.02

The total porosity of the porous sample was calculated as follows. First, the bulk density was calculated from the bulk volume and mass of the sample. Subsequently, the intrinsic density of the sample was determined using a pycnometer. The relative density of the sample was calculated from these values. Finally, the total porosity was defined as the inverse of the relative density. The estimated spinel conversion ratios of the porous samples were calculated on the basis of weight gain and accurate X-ray diffraction analysis (XD-D1, Shimazu Co. Ltd., Japan). The compressive strength of the porous samples was examined using an INSTRON 5582 (INSTRON Co. Ltd., Japan) device. The specific heat and thermal diffusivity were measured by a differential scanning calorimeter (DSC8230, Rigaku Co. Ltd., Japan) and a laser flash device (TC-7000, Optronics Co. Ltd, Japan), respectively, using the JIS R 1611 method. The micromorphology of the porous samples was observed using a scanning electron microscope (SEM: JEOL 5200, JEOL Co. Ltd., Japan). Three to five test pieces were used for each experimental condition.

3. Results and discussion

3.1. Porosity

Fig. 2 shows sample porosity vs. the number of solution treatments. The porosity of the samples decreased with increasing number of solution treatments. The porosity of a pure porous alumina body without solution treatment was approximately 72.5%. In contrast, after five solution treatments, the porosity of the samples decreased to 61.0% on average. Newly precipitated phases and/or the mass transport of alumina (sintering behavior) seemed to decrease the porosity. If spinel formation occurred, there would be a 5–7% volume expansion [4], which could also lead to a decrease in porosity.

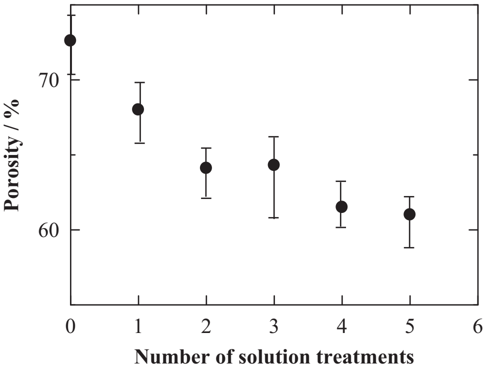

Fig. 2. Porosity of porous bodies vs. number of solution treatments.

3.2. Compressive strength

Fig. 3 shows the compressive strength of the samples vs. the number of solution treatments. By increasing the number of solution treatments, the compressive strength of the samples increased. After five solution treatments, the compressive strength reached 13.0 MPa. Generally, the mechanical strength of spinel and magnesia are lower than that of alumina [1]; therefore, the newly precipitated phase after solution treatment was not expected to increase the compressive strength. Thus, it was concluded that the alumina platelets became more strongly linked due to active mass transport with decreasing porosity, leading to increased compressive strength.

3.3. Ratio of conversion to spinel

Fig. 4 shows XRD patterns of samples with different numbers of solution treatments. As can be seen, no MgO was detected in any sample, which indicates that the initially precipitated MgO completely reacted with Al_2O_3 to form spinel during processing. Therefore, the ratio of conversion to spinel could be calculated from the sample weight gain according to the following chemical reaction:

$$MgO + Al_2O_3 = MgAl_2O_4 \quad (1)$$

Fig. 5 shows the conversion ratio to spinel vs. the number of solution treatments based on the weight gain of a porous Al_2O_3 sample. As shown in Fig. 4, the X-ray diffraction peaks corresponding to spinel increased with each additional solution treatment. After five solution treatments, the ratio of conversion to spinel was estimated to be 70–80%, according to the master curve for the spinel content of Al_2O_3. However, XRD analysis is very sensitive to the surface region of grains, so the spinel content tended to be overestimated when anisotropic alumina grains (platelets) were used. According to Fig. 5, only a 30% molar ratio of spinel was actually formed in a porous sample after five solution treatments. However, almost the entire surface of the alumina platelet grains seemed to be covered with spinel. Fig. 6 shows an SEM micrograph of a porous sample after five solution treatments. The surfaces

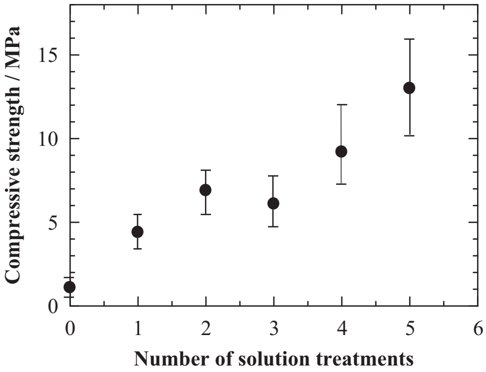

Fig. 3. Compressive strength of porous bodies vs. number of solution treatments.

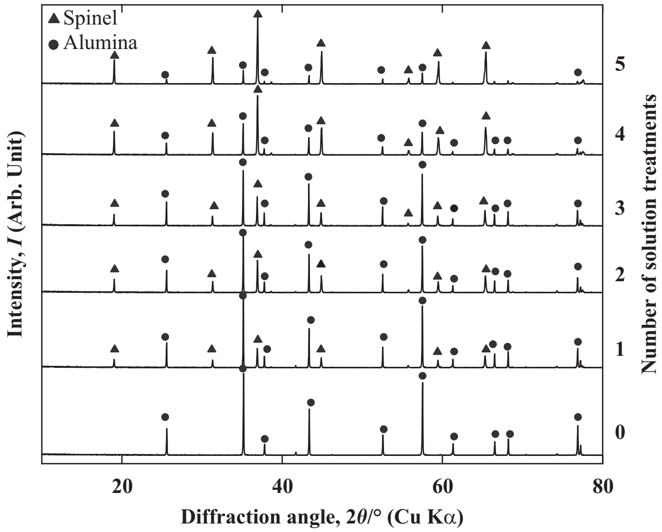

Fig. 4. XRD patterns of porous alumina bodies vs. number of solution treatments.

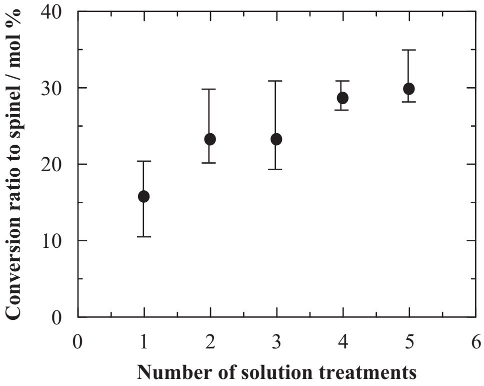

Fig. 5. Conversion ratio to spinel of the porous alumina bodies vs. number of solution treatments based on weight gain of the starting porous alumina.

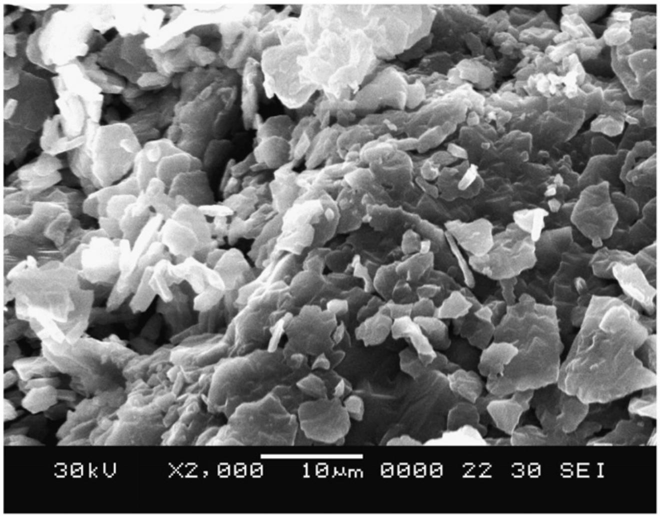

Fig. 6. SEM micrograph of a porous body after five solution treatments.

of the platelets were rough, but the overall platelet shape remained. This suggests that the alumina platelets were covered with the precipitated spinel. Therefore, the 10% decrease in porosity and tenfold increase in compressive strength after five solution treatments, as shown in Figs. 2 and 3, respectively, are thought to be caused by the occurrence of significant (active) mass transport of alumina as well as the formation of spinel, or, in other words, by alumina sintering.

3.4. Thermal conductivity

Generally, the thermal conductivity λ of a material is calculated from the following equation:

$$\lambda = \rho \mathrm{C}p\kappa \tag{2}$$

where ρ is the sample density, Cp is the specific heat, and κ is the thermal diffusivity. Cp and κ can be measured by DSC and a laser flash device, respectively. Fig. 7 shows the thermal conductivity of samples vs. the number of solution treatments over the temperature range from room temperature to 300 °C. With increasing temperature, the thermal conductivity of the porous samples decreased due to an increase in phonon–phonon interactions [14]. After one solution treatment, the thermal conductivity of the sample increased slightly from 3.7 $\mathrm{Wm^{-1}K^{-1}}$ of the pure phase to 3.9 $\mathrm{Wm^{-1}K^{-1}}$. With increasing solution treatments, the thermal conductivity of the sample decreased, finally reaching 1.8 $\mathrm{Wm^{-1}K^{-1}}$ after five solution treatments. In these porous samples, the pore diameter was several micrometers due to the size of the platelets. Furthermore, because the temperature remained below 300 °C, heat transfer by convection and radiation can be ignored, and the heat transfer was governed by conduction. Nait-Ali et al. suggested a thermal conductivity equation for porous materials with interconnected spherical pores [15]. In contrast, the authors believe that the thermal conductivity λ_o of porous ceramics in which spherical solid particles are interconnected to form percolations can be calculated from the following equation:

$$\lambda_o = 1/4[\lambda_s(3\upsilon_s-1)+\lambda_p(3\upsilon_p-1)+([\lambda_s(3\upsilon_s-1) + \lambda_p(3\upsilon_p-1)]^2+8\lambda_p\lambda_s)^{0.5}] \tag{3}$$

where υ_s and υ_p are the volume fractions of alumina and air filling the pores, respectively. The thermal conductivity λ_s of pure dense alumina and spinel is 32 and 16 $\mathrm{Wm^{-1}K^{-1}}$, respectively [1]. The thermal conductivity of air (pores) was estimated to be 0.025 $\mathrm{Wm^{-1}K^{-1}}$. Thus, the thermal conductivity of the porous alumina with 72.5% porosity before solution treatment was calculated to be 8.0 $\mathrm{Wm^{-1}K^{-1}}$. Furthermore, after five solution treatments, if the porous ceramic is composed of only spinel with 61.0% porosity, although the content of spinel was 30%, the thermal conductivity can be calculated to be 3.4 $\mathrm{Wm^{-1}K^{-1}}$. It is clear that the thermal conductivity of the porous bodies decreased with the volume fraction of spinel after solution treatment. However, both the calculated thermal conductivities were slightly higher than the corresponding experimental results. The card-house structure composed of platelets, the high porosity, and the existence of two different phases make it difficult to accurately predict the thermal conductivity. To perform more accurate calculations, Eq. (3) should be further modified.

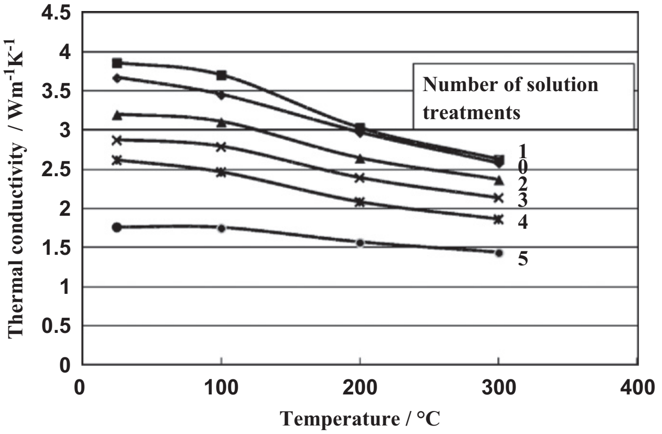

Fig. 7. Thermal conductivity of porous bodies vs. number of solution treatments at up to 300 °C.

After one solution treatment, the increase in thermal conductivity was considered to be caused by the formation of strong linkages between the platelets due to acceleration of the mass transport of alumina in the presence of MgO. Under these conditions, the main network linkage mode was thought to be alumina. After two solution treatments, the main network linkage mode changed to alumina–spinel, so the thermal conductivity began to decrease. After three solution treatments, a spinel–spinel network became dominant, so that the thermal conductivity decreased with further solution treatments. This spinel formation mechanism for different numbers of solution treatments is shown in Fig. 8. The final porous bodies had high porosity, high compressive strength, and low thermal conductivity, which would make them suitable for use as refractory materials.

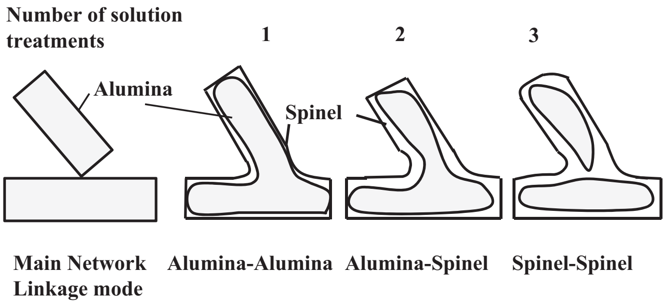

Fig. 8. Evolution of the spinel formation mechanism as the number of solution treatments is increased.

4. Conclusions

Initially, a porous alumina body with 72.5% porosity was fabricated by heating a compact composed of 85% alumina platelets, 10% corn starch as a pore former, and 5% fine alumina as a sintering additive at 1400 °C for 1 h. The resultant porous alumina was immersed in an 8 mol% magnesium nitrate solution for 1 h in vacuum, dried for 24 h in air, and reheated at 1400 °C for 2 h. This solution treatment was performed up to five times. With increasing solution treatments, the porosity decreased, the compressive strength increased, and the thermal conductivity decreased. After five solution treatments, the conversion ratio to spinel was calculated to be approximately 30% in molar ratio, while the remaining majority maintained the morphology of the alumina platelets. In addition, the porosity, compressive strength, and thermal conductivity of the final sample at room temperature were 61.0%, 13.0 MPa, and 1.8 $\mathrm{Wm^{-1}K^{-1}}$, respectively.

References

[1] J.F. Lynch, C.G. Ruderer, W.H. Duckworth, Engineering Properties of Selected Ceramic Materials, The American Ceramic Society, Columbus, Ohio, 1966.

[2] M. Sindel, N.A. Travitzky, N. Claussen, Influence of magnesium–aluminum spinel on the directed oxidation of molten aluminum alloys, Journal of the American Ceramic Society 73 (1990) 2615–2618.

[3] R.E. Carter, Mechanism of solid state reaction between MgO and Al_2O_3 and MgO and Fe_2O_3, Journal of the American Ceramic Society 44 (1961) 116–120.

[4] H.C. Park, Y.B. Lee, K.D. Oh, F.L. Riley, Grain growth in sintered $MgAl_2O_4$ spinel, Journal of Materials Science Letters 16 (1997) 1841–1844.

[5] L.B. Kong, J. Ma, H. Huang, $MgAl_2O_4$ spinel phase derived from oxide mixture activated by a high-energy ball milling process, Materials Letters 56 (2002) 238–243.

[6] R. Sarkar, S.K. Das, G. Banerjee, Effect of attrition milling on the densification of magnesium aluminate spinel, Ceramics International 25 (1999) 485–489.

[7] Y. Suyama, A. Kato, Characterization and sintering of Mg–Al spinel prepared by spray-pyrosis technique, Ceramics International 8 (1982) 17–21.

[8] C.R. Bickmore, K.F. Waldner, D.R. Treadwell, R.M. Laine, Ultra-fine spinel powders by flame spray pyrolysis of a magnesium aluminum double alkoxide, Journal of the American Ceramic Society 79 (1996) 1419–1423.

[9] C.-T. Wang, L.-S. Lin, S.-J. Yang, Preparation of $MgAl_2O_4$ spinel powders via freeze-drying of alkoxide precursors, Journal of the American Ceramic Society 75 (1992) 2240–2243.

[10] J. Katanic-Popovic, N. Miljevic, S. Zec, Spinel formation from coprecipitated gel, Ceramics International 17 (1991) 49–52.

[11] T. Shiono, K. Shiono, K. Miyamoto, G. Pezzotti, Synthesis and characterization of $MgAl_2O_4$ spinel powder from a heterogeneous alkoxide solution containing fine MgO powder, Journal of the American Ceramic Society 83 (2000) 235–237.

[12] I. Ganesh, Fabrication of magnesium aluminate ($MgAl_2O_4$) spinel foams, Ceramics International 37 (2011) 2237–2245.

[13] S. Hashimoto, A. Yamaguchi, Synthesis of α-Al_2O_3 platelets using sodium sulfate flux, Journal of Materials Research 14 (1999) 4667–4672.

[14] D.S. Smith, S. Grandjean, J. Absi, S. Kadiebu, S. Fayette, Grain-boundary thermal resistance in polycrystalline oxides: alumina, tin oxide and magnesia, High Temperature-High Pressure 35/36 (2002) 93–99.

[15] B. Nait-Ali, K. Haberko, H. Vesteghem, J. Abis, D.S. Smith, Thermal conductivity of highly porous zirconia, Journal of the European Ceramic Society 26 (2006) 3567–3574.